Published in final edited form as:
Cell. 2011 November 11; 147(4): . doi:10.1016/j.cell.2011.10.022.

Systematic Discovery of TLR Signaling Components Delineates Viral-Sensing Circuits

Nicolas Chevrier[1,2,3,4], **Philipp Mertins**[1], **Maxim N. Artyomov**[1,6], **Alex K. Shalek**[7], **Matteo Iannacone**[5,9], **Mark F. Ciaccio**[8], **Irit Gat-Viks**[1,6,10], **Elena Tonti**[5,9], **Marciela M. DeGrace**[1,2,3], **Karl R. Clauser**[1], **Manuel Garber**[1], **Thomas M. Eisenhaure**[1,2], **Nir Yosef**[1,6], **Jacob Robinson**[7], **Amy Sutton**[7], **Mette S. Andersen**[7], **David E. Root**[1], **Ulrich von Andrian**[5], **Richard B. Jones**[8], **Hongkun Park**[7], **Steven A. Carr**[1], **Aviv Regev**[1,6,^], **Ido Amit**[1,2,3,6,11,^,†], and **Nir Hacohen**[1,2,3,^,†]

[1] Broad Institute of MIT and Harvard, 7 Cambridge Center, Cambridge, MA 02142

[2] Center for Immunology and Inflammatory Diseases, Massachusetts General Hospital, Charlestown, MA 02129

[3] Department of Medicine, Harvard Medical School, Boston, MA 02115

[4] Graduate Program in Immunology, Division of Medical Sciences, Harvard Medical School, Boston, MA 02115

[5] Immune Disease Institute and Department of Pathology, Harvard Medical School, Boston, MA 02115

[6] Howard Hughes Medical Institute, Department of Biology, MIT, Cambridge, MA 02142

[7] Departments of Chemistry and Chemical Biology, and of Physics, Harvard University, Cambridge, MA 02138

[8] The Ben May Department for Cancer Research and the Institute for Genomics and Systems Biology, The University of Chicago, Chicago, Illinois, USA

[9] Division of Immunology, Infectious Diseases and Transplantation, San Raffaele Scientific Institute, Milan, Italy

SUMMARY

Deciphering the signaling networks that underlie normal and disease processes remains a major challenge. Here, we report the discovery of signaling components involved in the Toll-like receptor (TLR) response of immune dendritic cells (DCs), including a previously unkown pathway shared across mammalian antiviral responses. By combining transcriptional profiling, genetic and small molecule perturbations, and phosphoproteomics, we uncover 35 signaling regulators, including 16 known regulators, involved in TLR signaling. In particular, we find that Polo-like kinases (Plk) 2 and 4 are essential components of antiviral pathways *in vitro* and *in vivo*, and

[†] To whom correspondence should be addressed. ido.amit@weizmann.ac.il, nhacohen@partners.org.
[10]Current address: Dept. of Cell Research and Immunology, George S. Wise Faculty of Life Sciences, Tel Aviv University, Tel Aviv 69978, Israel
[11]Current address: Department of Immunology, Weizmann Institute of Science, Rehovot 76100, Israel
[^]These authors contributed equally to this work

ACCESSION NUMBERS

Complete microarray data sets are available in the NCBI Gene Expression Omnibus (accession number GSE28520). Proteomics raw data are in the the Tranche data repository (https://proteomecommons.org/tranche/, hash: HTWY5ZeSLM1hyYEyfEiJREkgLXs6BZxCczuixy9XjULsync5HCkXx/8gB7nZKpGocwOnt8vOk/Q3cpbPh/ycD/2LT0AAAAAAAAAuEg== and passphrase: SpSTB6vceSUKeNqefq59.)

activate a signaling branch involving a dozen proteins among which is Tnfaip2, a gene associated with autoimmune diseases but whose role was unknown. Our study illustrates the power of combining systematic measurements and perturbations to elucidate complex signaling circuits and discover potential therapeutic targets.

INTRODUCTION

Signaling networks detect and respond to environmental changes, and defects in their wiring can contribute to diseases. For example, Toll-like receptors (TLRs) sense microbial molecules and trigger signaling pathways critical for host defense (Takeuchi and Akira, 2010). Genetic defects in components of the TLR and other pathogen-sensing pathways have been linked to human diseases. Hence, rational targeting of these pathways should help in better manipulating immune responses associated with infections, autoimmunity, and vaccines (Hennessy et al., 2010).

However, despite extensive studies, many components of TLR and other biological networks are unknown, and many genes associated with disease have not been assigned to a function or a pathway. A key challenge is thus to systemically dissect mammalian signaling networks, by determining the functions of their components and placing them within pathways. Previously, we introduced an integrated experimental and computational approach to decipher the TLR transcriptional network of immune dendritic cells (DCs) (Amit et al., 2009), allowing us to identify transcriptional regulators and to define their impact on TLR responses in DCs. For example, we found a host of cell cyle regulators – Rbl1, Rb, Myc, Jun, and E2fs – that are required for antiviral transcriptional responses in non-dividing DCs.

Here, we adapt and expand this approach to the discovery and validation of TLR signaling components in DCs (**Figure S1**). **First**, to identify candidate components, we rely on transcriptional feedbacks, whereby a signaling circuit regulates the transcript levels of genes encoding some, but not all, of its components (Amit et al., 2007; Fraser and Germain, 2009; Freeman, 2000). **Second**, we perturb these candidates with shRNAs, and measure the effects on a representative signature of >100 TLR-activated genes. **Third**, we use functional phosphoproteomics to expand the pathway's scope to components whose mRNA levels may be unchanged upon TLR activation. Applying this approach iteratively, we discovered 19 functional components, including a signaling arm mediated by two Polo-like kinases (Plk2 and 4) that participate in regulating well-established host antiviral pathways.

RESULTS

Transcripts for signaling components are regulated upon TLR stimulation

To identify candidate components of pathogen-sensing pathways, we used genome-wide mRNA profiles, previously measured at 10 time points along 24 hours following stimulation of primary bone marrow-derived DCs (BMDCs) with lipopolysaccharide (LPS; TLR4 agonist), polyinosinic:polycytidylic acid (poly(I:C); recognized by TLR3 and the cytosolic viral sensor MDA-5), or Pam3CSK4 (PAM; TLR2 agonist) (Amit et al., 2009). These three TLRs activate transcriptional programs referred to here as “inflammatory” (TLR2), “antiviral” (TLR3), or both (TLR4) (**Figure 1A**) (Amit et al., 2009; Doyle et al., 2002).

Our analysis uncovered 280 genes annotated as known or putative signaling molecules that were differentially expressed following stimulation: 115 kinases, 69 phosphatases, and 96 other regulators, such as adaptors and scaffolds (Figure 1B and Table S1, and Experimental Procedures). These 280 genes were enriched for canonical pathways of the TLR network

such as MAP kinase ($P < 1.22\times10^{-15}$, overlap 25/87, hypergeometric test), TLR (*e.g.*, Myd88, Traf6, Irak4, Tbk1; $P < 8.43\times10^{-12}$, 21/86), and PI3K ($P < 2.58\times10^{-8}$, 11/33) pathways, as well as the PYK2 pathway ($P < 3.12\times10^{-10}$, 12/29), which was recently associated with the TLR system (Wang et al., 2010). Overall, 94 of the 280 genes (33%) were associated with the TLR network in the literature (**Table S1**), supporting the validity of our candidate selection strategy. The remaining 186 genes (67%) represent candidate TLR components. To test their putative function in TLR signaling, we selected a subset of 23 candidates based on their strong differential expression, and to proportionally represent the five main induced expression clusters (**Figure 1B and 1C**). We also selected 6 canonical TLR components (Myd88, Mapk9, Tbk1, Ikbke, Tank, and Map3k7) as benchmarks (**Figure 1A and 1D**).

A perturbation strategy places uncharacterized signaling components within the antiviral and inflammatory pathways

We perturbed our 6 positive controls and 17 of the 23 candidates in BMDCs using shRNA-encoding lentiviruses (six candidates showed poor knockdown efficiency) (**Table S1**). We stimulated the cells with LPS, and measured the effect of gene silencing on the mRNA levels of 118 TLR response signature genes, representing the inflammatory and antiviral programs, using a multiplex mRNA counting method (**Figure 2A**). Notably, the expression of the 118-genes was not affected in BMDCs transduced with lentivirus compared to untransduced cells (Amit et al., 2009). We determined statistically significant changes in the expression of signature transcripts upon individual knockdowns based on comparison to 10 control genes, whose expression remains unchanged upon TLR activation, and to control shRNAs (**Experimental Procedures**). Finally, we associated signaling molecules and downstream transcriptional regulators that may act in the same pathway by comparing the perturbational profiles of the 23 signaling molecules (6 canonical and 17 candidates) to each other and to those of the 123 transcriptional regulators (including transcription and chromatin factors and RNA-binding proteins) previously tested (**Figure 2 and Figure S2 and Table S2**) (Amit et al., 2009).

Perturbing 5 of the 6 canonical signaling molecules strongly affected the expression of TLR signature genes, consistent with their known roles (**Figure 2A and Table S2**) and validating our approach. For example, perturbing Myd88, a known inflammatory adaptor, specifically abrogated the transcription of inflammatory genes (*e.g.*, Cxcl1, Il1a, Il1b, Ptgs2, Tnf; **Figure 2A**), similar to perturbations of downstream inflammatory transcription factors (*e.g.*, Nfkb1, Nfkbiz; **Figure 2B**). In addition, Tank acted as a negative regulator of a subset of antiviral genes (**Figure 2A**), as expected (Kawagoe et al., 2009), and Tbk1 knockdown affected both antiviral and inflammatory outputs (**Figure 2A**), consistent with findings that Tbk1 regulates NF-κB complexes (Barbie et al., 2009; Chien et al., 2006). Notably, Ikbke (IKK-ε) knockdown did not affect our gene signature, consistent with previous observations that IKK-$\varepsilon^{-/-}$ DCs respond normally to LPS and viral challenges (Matsui et al., 2006). Thus, IKK-ε may either be not functional or redundant in our system.

All of the 17 candidate signaling molecules tested, except Plk2 (discussed below), affected at least 6 of the 118 genes (on average, 16.6 targets±10.4SD), and 12 affected more than 10% of the genes (**Figure S2A and S2D**). Notably, perturbations of these 17 candidates did not affect BMDC differentiation (88.3% ± 6.8 SD of $CD11c^+$ cells; **Table S1**). These effects are comparable to those of known signaling molecules and transcriptional regulators in this system (**Figure S2B-E**). For example, the receptor tyrosine kinase Met, not previously associated with TLR signaling, affected a number of signature genes similar to Tbk1 (**Figure S2C and S2D**), in both the inflammatory and antiviral programs (**Figure 2A**). Conversely, both the phosphatase Ptpre and the adaptor Socs6 positively regulated the

inflammatory program, while negatively regulating some antiviral genes (**Figure 2B**). Of the 17 candidates tested when we originally conducted this screen, 10 have subsequently been reported in other studies as functional in the TLR system (**Table S1**), providing an independent confirmation. For example, Map3k8 knockdown affected here both inflammatory and antiviral target genes (**Figure 2A**), consistent with its reported role in the TLR pathways based on *Sluggish* mice (Xiao et al., 2009).

We identified both primary (*e.g.*, Myd88) and secondary (*e.g.*, Stat1) mediators of TLR responses. While secondary mediators are not part of the initial intracellular signaling cascade, they are important physiological components of the TLR response and their pertubation can lead to similar phenotypic outcomes as that of primary components. For example, the receptor tyrosine kinase Mertk acted as both a positive and negative regulator of some inflammatory and antiviral genes (e.g., Ifnb1) respectively (**Figure 2A**), consistent with its reported role as a secondary inhibitor of the TLR pathways (Rothlin et al., 2007).

Crkl modulates JNK-mediated antiviral signaling in the TLR network

Among the 17 candidate signaling proteins, perturbation of the tyrosine kinase adaptor Crkl decreased expression of 13% of the signature genes, especially antiviral ones (**Figure 2A and Figure S2D**). Crkl belongs to several signaling pathways, including early lymphocyte activation (Birge et al., 2009), but has not been associated with the TLR network. Crkl's perturbation profile closely resembled those of known antiviral regulators, most notably Jnk2 (Mapk9; Chu et al., 1999) (**Figure 2A and 3A**). Indeed, when $Crkl^{-/-}$ DCs were stimulated with LPS, the expression of antiviral cytokines (Cxcl10, Ifnb1) was strongly reduced (**Figure 3B, left and middle**), but that of an inflammatory cytokine (Cxcl1) was unaffected (**Figure 3B, right**).

To test whether Crkl is a primary component of the TLR pathway, we measured if Crkl phosphorylation is rapidly modified after TLR signaling initiation. Using SILAC-based (Ong et al., 2002) quantitative phosphoproteomics, we identified and quantified 62 phospho-tyrosine (pTyr)-containing peptides from BMDCs stimulated with LPS for 30 minutes (**Figure 3C and Table S3 and Experimental Procedures**). Of these 62 phosphopeptides, 7 and 9 were significantly up- or down-regulated, respectively (**Figure 3C and Table S3**). A phosphopeptide derived from Crkl (Y132) – one of the top-six induced phosphopeptides – was induced 2.1 fold (**Figure 3C**). This indicates that Crkl is likely activated directly downstream of TLR4 signaling.

Several lines of evidence suggest that Crkl acts through Jnk2 (Mapk9) signaling. **First**, the MAP kinase Jnk2 (Mapk9) is co-regulated at the phosphorylation level with Crkl upon LPS stimulation (**Figure 3C**). **Second**, the Crk adaptor family – including CrkI, CrkII, and Crkl – has been shown to modulate Jnk activity in growth factor and IFN signaling (Birge et al., 2009; Hrincius et al., 2010). **Third**, the perturbation profiles of Mapk9 and Crkl are strikingly similar (**Figure 3A**). These observations suggest that Crkl modulates Jnk-mediated antiviral signaling in the TLR4 pathway, providing a possible explanation for why the NS1 protein of influenza A virus may target Crkl (Heikkinen et al., 2008; Hrincius et al., 2010).

Polo-like kinases are critical activators of the antiviral program

To discover potential drug targets among our 17 candidates, we next focused on Polo-like kinase (Plk) 2, a well-known cell cycle regulator and drug target (Strebhardt, 2010). The roles of Plks in non-dividing, differentiated cells are poorly defined (Archambault and Glover, 2009; Strebhardt, 2010). We have previously shown that transcriptional regulators of cell cycle processes (*e.g.*, Rbl1, Rb, Myc, Jun, E2fs) are co-opted to function in the

antiviral responses in DCs (Amit et al., 2009). However, neither knockdown (**Figure 2A**) nor knockout (**Figure S3A**) of Plk2 in BMDCs had any effect on the TLR response. We hypothesized that this could be due to functional redundancy with another Plk, since Plk4 mRNA was induced in DCs similarly to Plk2 (**Figure 4A**), albeit at a lower amplitude (and thus was below our threshold for inclusion in the initial candidate list). Interestingly, functional redundancy between Plk2 and 4 has been suggested to account for the viability of Plk2-deficient mice (Strebhardt, 2010), and Plk2 and 4 have been reported to function together in centriole duplication (Chang et al., 2010; Cizmecioglu et al., 2008).

To test our hypothesis, we simultaneously perturbed Plk2 and 4 in BMDCs using two independent mixes of different pairs of shPlk2/shPlk4 (**Figure S3B and Experimental Procedures**). We observed a significant and specific decrease in the expression of 21 antiviral genes (**Figure 4B**). For example, the antiviral cytokines Ifnb1 and Cxcl10 mRNAs were decreased, whereas the expression of the inflammatory gene Cxcl1 and almost all inflammatory signature genes remained unaffected (**Figure 4C**). Two recent reports suggested a role for Plk1 alone as a negative regulator of MAVS (Vitour et al., 2009) and NF-κB (Zhang et al., 2010) in cell lines. However, knockdown of either Plk1 or Plk3 in BMDCs did not affect the TLR transcriptional response (**Figure S3C and Table S2**). Notably, BMDC viability was unaffected by lentiviral shRNA transduction targeting Plk1, 2, 3 or 4 individually, or Plk2 and 4 together (based on mRNA levels of control genes; **Table S2**). Thus, in BMDCs, Plk2 and 4, but likely not Plk1 or 3, are critical regulators of antiviral but not cell cycle pathways.

A small molecule inhibitor of Plks represses antiviral gene expression and IRF3 translocation in DCs

We next targeted Plks in BMDCs using BI 2536, a commercial pan-specific Plk small molecule inhibitor (**Steegmaier et al., 2007**). We compared genome-wide mRNA profiles from BMDCs treated with either BI 2536 or DMSO vehicle before stimulation with LPS or poly(I:C) (**Experimental Procedures**). BI 2536 treatment repressed mostly antiviral gene expression compared to DMSO (99/193 genes in response to poly(I:C), $P < 1\times10^{-71}$, hypergeometric test; 67/194 in response to LPS; **Table S4**). The 311 unique LPS- and/or poly(I:C)-induced genes that are repressed by BI 2536, are significantly enriched for genes related to cytokine signaling (*e.g.*, IL-10, type I IFNs, IL-1), TLR signaling, and DC signaling, and for GO processes related to defense and immune responses (**Figure S4A**). Consistent with the array data, BI 2536 strongly inhibited the expression of 12 well-studied antiviral genes whereas inflammatory gene expression remained largely unaffected in DCs stimulated with LPS, poly(I:C), or Pam3CSK4, as measured by qPCR (**Figure 4D**).

BI 2536 reduced the mRNA levels of Cxcl10 and Ifnb1 (by qPCR) and of secreted IFN-β in a dose-dependent manner, while Cxcl1 expression was not significantly affected (**Figure S4B and S4C**). Importantly, BI 2536 treatment pre-stimulation neither impacted the viability nor the cell cycle state of BMDCs (**Figure S4D and S4E**), suggesting that Plk inhibition does not act through cell cycle effects. Consistent with our shRNA and BI 2536 perturbations, two other pan-Plk inhibitors – structurally unrelated to BI 2536 – also repressed Ifnb1 and Cxcl10 expression without affecting Cxcl1 (**Figure S4F**). This strongly suggests that the effects induced by these perturbations are due to Plks inhibition, and not off-target effects. Furthermore, we observed a similar inhibitory effect of BI 2536 on Ifnb1 induction in Ifnar1$^{-/-}$ and wild-type BMDCs, demonstrating that Plks act directly downstream of TLR activation, and not in an autocrine/paracrine feedback loop mediated by IFN receptor signaling (**Figure S4G**). This is consistent with a recent phosphoproteomic study reporting an enrichment for Plk substrates as early as 15 min after LPS stimulation in macrophages (Weintz et al., 2010).

We next used confocal microscopy to monitor the effect of BI 2536 on the subcellular localization of IRF3, a key antiviral transcription factor. To more effectively deliver the drug, we plated BMDCs on vertical silicon nanowires (Shalek et al., 2010) pre-coated with BI 2536 pre-stimulation. Nanowires alone had no effect on the TLR response (**Figure 5A and Figure S5A**). BI 2536 inhibited IRF3 nuclear translocation in a dose-dependent manner upon poly(I:C) or LPS stimulation, whereas the control JNK inhibitor SP 600125 had no effect (**Figure 5B and 5C, and Figure S5B**). On the other hand, BI 2536 did not affect NF-κB p65 localization (**Figure 5D and 5E**). Notably, IRF3 translocation was also decreased when delivering BI 2536 in solution, but to a lesser extent compared to nanowire-mediated delivery (**Figure S5C**), highlighting the utility of highly efficient drug delivery methods to induce homogeneous effects in single-cell assays. Altogether, these results place Plk2 and 4 as critical regulators of the antiviral program, upstream of a major antiviral transcription factor.

Plks are essential for activation of all well-established IFN-inducing pathways in conventional and plasmacytoid DCs

DCs can be broadly categorized into two major subtypes – conventional and plasmacytoid DCs – each relying on distinct mechanisms to induce type I IFNs and antiviral gene expression (Blasius and Beutler, 2010). In conventional DCs (cDCs), antiviral responses are activated through TLR4/3 signaling (via TRIF), or through the cytosolic sensors RIG-I or MDA-5 (via MAVS) (**Figure 6A**). In plasmacytoid DCs (pDCs; specialized IFN-producing cells), the antiviral response depends solely on endosomal TLR7 and 9 that signal via MYD88 (**Figure 6A**) (Blasius and Beutler, 2010; Takeuchi and Akira, 2010).

BI 2536 treatment showed that Plks are essential for the viral-sensing pathways in both cDCs and pDCs. **In cDCs**, BI 2536 inhibited the transcription of antiviral genes (Ifnb1 and Cxcl10) upon infection with each of four viruses: vesicular stomatitis virus (VSV, **Figure 6B, top**), Sendai virus (SeV; **Figure S6A top**), or Newcastle disease virus (NDV; **Figure S6A bottom**), all three sensed through RIG-I, and encephalomyocarditis virus (EMCV), sensed through MDA-5 (**Figure 6B, bottom and Experimental Procedures**). Notably, BI 2536 neither affected the mRNA level of Cxcl1 (an inflammatory cytokine) in any of the four cases, nor affected the response to heat-killed *Listeria monocytogenes*, a natural TLR2 agonist (**Figure 6B and Figure S6A and S6B**). **In pDCs**, BI 2536 treatment nearly abrogated the transcription of mRNAs for the antiviral cytokines Ifnb1, Ifna2, and Cxcl10 after stimulation with type A CpG oligonucleotides (CpG-A), or infection with EMCV, sensed by TLR9 and 7, respectively (**Figure 6C, Figure S6C, and Experimental Procedures**). Conversely, in pDCs stimulated with CpG-B – a ligand known to activate inflammatory pathways but not IFN-inducing pathways – BI 2536 treatment decreased Cxcl10 mRNA, while moderately increasing Cxcl1 mRNA (**Figure 6C**). Finally, of our 118 signature genes, BI 2536 repressed genes induced by CpG-A alone or by both CpG-A and -B, while having a minor effect, if any, on CpG-B-specific genes in pDCs (**Figure 6D and Table S5**). These findings may help reveal the poorly characterized molecular determinants of IFN production in pDCs (Reizis et al., 2011), and demonstrate a critical role for Plks across all well-known IFN-inducing pathways.

Plks are essential in the control of host antiviral responses

To assess the impact of Plk inhibition on the outcome of viral infection, we infected primary mouse lung fibroblasts (MLFs) with influenza virus. BI 2536-treated MLFs infected with influenza failed to produce interferon (**Figure 6E**), and showed elevated replication of both wild-type (PR8) and poorly-replicating mutant (ΔNS1) viruses (**Figure 6F**). The reduced interferon response was not due to drug-induced toxicity (**Figure 6G**).

Next, we tested the effects of Plk inhibition in virally infected mice. BI 2536 exhibits good tolerability in mice (**Steegmaier et al., 2007**) and humans (Mross et al., 2008), and is currently in Phase II clinical trials as an anti-tumor agent in several cancers (Strebhardt, 2010). Given its efficacy and safety *in vivo*, we tested whether BI 2536 would also affect the response to viral infection in animals. In mice infected with VSV, BI 2536 strongly suppressed mRNA production in popliteal lymph nodes for type I IFNs (Ifnb1, Ifna2) and Cxcl10, but did not affect Cxcl1 mRNA induction (all compared to vehicle control; **Figure 6H and Figure S6D**). Concomitantly, VSV replication in the lymph node rapidly increased as reflected by elevated VSV RNA levels (**Figure 6I**), comparable to the observed phenotype of VSV-infected Ifnar1$^{-/-}$ mice (Iannacone et al., 2010). Because in the VSV model used here type I IFNs are produced by both infected CD169^{+} subcapsular sinus macrophages and pDCs (Iannacone et al., 2010), we cannot distinguish whether Plk inhibition affects macrophages, pDCs, or both. Nevertheless, our results confirm the physiological importance of Plks in the host antiviral response in both *ex vivo* primary MLFs and *in vivo* mouse lymph nodes.

Plks affect the phosphorylation of dozens of proteins post-LPS stimulation, including known and candidate antiviral regulators

We next sought to discover the signaling pathways between Plks and antiviral gene transcription. We used MicroWestern Arrays (MWAs) (Ciaccio et al., 2010) to measure changes in the phosphorylation and protein levels of 20 and 6 TLR pathway proteins, respectively, in BMDCs at each of 12 combinations of four time points (0, 20, 40, 80 min after LPS stimulation) and three perturbations (vehicle control, BI 2536, and negative control JNK inhibitor SP 600125) (**Table S6**). While LPS stimulation alone led to the expected changes (*e.g.*, early peak of phosphorylation for ERK1/2, p38, and Mapkapk2, and rapid degradation of IκBα; **Figure 7A**), BI 2536 surprisingly did not cause any significant changes (**Figure 7A and Figure S7A and S7B**). We therefore hypothesized that Plks could affect previously unrecognized regulators of IFN-inducing pathways and/or known regulators with no existing antibodies to specific phosphosites.

Next, we used SILAC-based unbiased phosphoproteomics (**Figure 7B top**) (Villen and Gygi, 2008) to compared the levels of phospho-tyrosine, -threonine and -serine peptides following stimulation with LPS (for 30 or 120 min) in BMDCs pre-treated with BI 2536 versus those treated with vehicle (DMSO). We identified and quantified 5,061 and 5,997 phosphopeptides after 30 and 120 minutes, respectively, for a total of 10,236 individual phosphosites (**Figure 7B and Table S6**). BI 2536 substantially affected the TLR phosphoproteome, leading to a significant ($P < 0.001$) change in the level of 510 phosphopeptides derived from 413 distinct proteins (**Figure 7B and Table S6**). Further supporting our results, 35% (2489/7018) of the phospho-sites we identified were recently reported in mouse bone marrow-derived macrophages treated with LPS (**Figure S7C, left**) (Weintz et al., 2010), and 483 of our phosphosites were among 1858 sites (26%) reported in a phosphoproteomic study of LPS signaling in a macrophage cell line (**Figure S7C, left**) (Sharma et al., 2010). A comparison of the phosphosites of known kinases showed similar overlaps between the three studies (**Figure S7C, right**).

The Plk-dependent phosphoproteins include several known regulators of antiviral pathways (*e.g.*, Prdm1, Fos, Unc13d) (Crozat et al., 2007; Keller and Maniatis, 1991; Takayanagi et al., 2002), as well as many additional protein candidates with no previously known function in viral sensing (**Figure 7B and Table S6**). Notably, proteins involved in the TBK1/IKK-ε/IRF3 axis were detected and quantified, but their phosphorylation levels were unchanged upon Plk inhibiton (**Table S6**), consistent with the MicroWestern array data. Conversely, Plk inhibition with BI 2536 decreased the phosphorylation levels of cell cycle regulators of

the Jun family of transcriptional regulators (*i.e.*, Jund) that we previously found to be co-opted by antiviral pathways (Amit et al., 2009). BI 2536 treatment also decreased the phosphorylation levels of the mitotic kinases Nek6 and Nek7 (**Figure 7B**). The recent observation that the phosphorylation Nek6 substrates are increased following LPS stimulation in macrophages (Weintz et al., 2010) indirectly corroborates our finding that Nek6 may be active in TLR signaling. To test the role of these Plk-dependent candidates, we returned to our shRNA perturbation-based approach.

Plk-dependent phosphoproteins affect the antiviral response

We perturbed 25 Plk-dependent phosphoproteins (**Table S7**), using shRNA perturbation in BMDCs followed by qPCR and TLR gene signature measurements. These candidates satisfied three criteria: (**1**) there was no prior knowledge of their function in viral sensing pathways; (**2**) their phosphoprotein levels were consistently up- or down-regulated upon BI 2536 treatment (in two independent experiments); and (**3**) they had detectable mRNA expression and/or differential expression upon stimulation.

Of the 18 phosphoproteins showing efficient knockdown, 11 caused a significant decrease in Ifnb1 mRNA levels with a single shRNA (Sash1, Dock8, Nek6, Nek7, Nfatc2, and Ankrd17; **Figure S7D**), or with two independent shRNAs (Tnfaip2, Samsn1, Arhgap21, Mark2, and Zc3h14; **Figure S7E**). Decrease in Cxcl10 expression was less prominent, consistent with our previous observations of BI2536's weaker effect on this cytokine during LPS stimulation (**Figure S7D and S7E, far right panels**). Each of the 11 Plk-dependent phosphoproteins tested affected at least 9 targets in the 118-gene signature (on average, 39 targets ± 30 SD; **Figure 7C**), and 9 affected more than 10% of the targets in the TLR gene signature (**Figure 7C**).

9 of the 11 Plk-dependent phosphoproteins affected the TLR signature comparably to major antiviral regulators (**Figure 7D**). For example, the knockdown profiles of Samsn1, Dock8, and Sash1 were closely correlated to those of Stat and Irf family members (**Figure 7D**), and those of Tnfaip2 and Zc3h14 were most correlated to the Plk2/4 double knockdown. Interestingly, Tnfaip2, a protein of unknown molecular function, has been associated with rheumatoid arthritis and autoimmune myocarditis in genome-wide association studies (Wellcome Trust Case Control Consortium, 2007; Kuan et al., 1999). Our findings provide a potential molecular context for this disease association.

DISCUSSION

Using an integrative strategy combining transcriptomics, genetic and chemical perturbations, and unbiased phosphoproteomics, we established a role for Plks in host defense pathways inducing type I IFNs, likely by controlling the phosphorylation and activity of a module of at least 11 components (**Figure 7E**). Our findings and approach open up several avenues for future investigations.

Consistent with our finding that cell cycle transcription factors play a role in antiviral responses (Amit et al., 2009), we identified several cell cycle kinases (Plks, Neks) as important regulators of these responses. Despite extensive studies on the role of Plk1 in mitosis, the functions of its paralogs – Plk2, 3, and 4 – are poorly defined (Strebhardt, 2010). While they are less essential than Plk1 in regulating cell division, their roles in non-dividing cells such as neurons are emerging (Archambault and Glover, 2009; Seeburg et al., 2005). Interestingly, silencing of both Plk2 and 4 was required to reveal their importance in antiviral responses, highlighting the necessity of epistasis analysis in studying mammalian signaling networks. While it is currently not feasible to screen for genetic interactions at a genome-wide scale, it will be interesting to develop innovative approaches to uncover them.

BI 2536 blocked the nuclear translocation of IRF3 without affecting its phosphorylation level (based on MicroWestern arrays and phosphoproteomics). A similar phenomenon has been reported for NF-kB (Ye et al., 2011). This suggests that IRF3 translocation in our system is likely to be regulated by a mechanism that does not impact phosphorylation.

Furthermore, Plk inhibition suppresses type I IFN production *in vivo* during viral infection – a finding which has potential clinical implications. Indeed, disease activity in patients with Systemic Lupus Erythematosus (SLE) correlates with IFN expression signatures (Banchereau and Pascual, 2006), and lupus-prone mice exhibit reduced symptoms upon treatment with a dual inhibitor of TLR7 and 9 (Barrat and Coffman, 2008) or deletion of the IFN receptor (Santiago-Raber et al., 2003). Thus, testing the effect of BI 2536 on a mouse model of lupus will be key to assess the potential therapeutic implications of Plk inhibition for SLE.

Our approach may be applicable for characterizing the functions of genes reported in genome-wide association studies (*e.g.*, Tnfaip2), for uncovering potential therapeutic targets (*e.g.*, Plks), and for re-purposing existing small molecules in new physiological contexts (*e.g.*, using the cancer drug BI 2536 to repress innate immune responses). The vast public compendia of microarray data could serve as starting points for identification of relevant signaling components in diverse biological systems, followed by perturbations and signature measurements. Nevertheless, since the mRNAs corresponding to many pathway components do not change upon pathway activation, our approach is far from exhaustive. Combination of our perturbation-based approach with large-scale biochemical measurements (*e.g.*, post-translational modifications, protein-protein interactions), will lead to more comprehensive, integrated maps of signaling and transcriptional networks.

EXPERIMENTAL PROCEDURES

Cells and mouse strains

Bone marrow-derived DCs were generated from 6-8 week old female C57BL/6J mice, Crkl mutant mice (Jackson Laboratories), Plk2$^{-/-}$ mice (Elan Pharmaceuticals), or Ifnar1$^{-/-}$ mice (gift from K. Fitzgerald). Primary mouse lung fibroblasts (MLFs) were from C57BL/6J mice.

Viruses

Sendai virus (SeV) strain Cantell and Encephalomyocarditis virus (EMCV) strain EMC (ATCC), Newcastle disease virus (NDV) strain Hitchner B1 (gift from A. Garcia-Sastre), and vesicular stomatitis virus (VSV) strain Indiana (U. von Andrian), were used for infections. Influenza A virus strain A/PR/8/34 and ΔNS1 were grown in Vero cells, and virus titers from MLF supernatants was quantified using 293T cells transfected with a vRNA luciferase reporter plasmid.

Reagents

TLR ligands were from Invivogen (Pam3CSK4, ultra-pure *E. coli* K12 LPS, ODN 1585 CpG type A, and ODN 1668 CpG type B) and Enzo Life Sciences (poly(I:C)). Heat-killed *Listeria monocytogenes* (HKLM) was from Invivogen. Polo-like kinase inhibitors were from Selleck (BI 2536), Sigma (GW843682X), and Chembridge (Poloxipan). SP 600125 (Jnk inhibitor) was from Enzo Life Sciences.

mRNA isolation, qPCR, and microarrays

Total or polyA+ RNA was extracted and reverse transcribed prior to qPCR analysis with SYBR Green (Roche) in triplicate with GAPDH for normalization. For microarray analysis, Affymetrix Mouse Genome 430A 2.0 Array were used.

shRNA knockdowns

High titer lentiviruses expressing shRNAs were obtained from The Broad RNAi Platform and used to infect BMDCs as previously described (Amit et al., 2009).

mRNA measurements on nCounter

5×10^4 bone marrow-derived DCs were lysed in RLT buffer (Qiagen) with 1% β-ME. 10% of the lysate was used for mRNA counting using the nCounter Digital Analyzer (NanoString) and a previously generated CodeSet of 118 genes (Amit et al., 2009). To score target genes whose expression is significantly affected by shRNA perturbations, we used a fold threshold corresponding to a false discovery rate (FDR) of 2%. Heatmaps and distance matrix analyses were generated using the Gene-E software (http://www.broadinstitute.org/cancer/software/GENE-E/).

Detection of regulated signaling genes

We identified differentially regulated signaling components (*i.e.*, kinases, phosphatases, and signaling adaptors or scaffolds) based on probesets reproducibly displaying at least 1.7-fold up- or down-regulation in at least one time point, compared to unstimulated controls, using our previously published microarray dataset (NCBI GEO GSE17721, Amit et al., 2009).

Nanowire-mediated drug delivery and microscopy

BMDCs were plated on top of etched silicon nanowires (Si NWs) coated with small molecules. After 24 hours, cells were stimulated and processed for immunofluorescence analysis by confocal microscopy.

VSV infection model

8-week old C57BL/6 male mice received 500 μg of BI 2536 (or vehicle) intravenously, and 50 μg into the footpad 3 hours before and 2 hours after infection with 10^6 pfu of VSV into the footpad. Mice were sacrificed 6 hours post-infection and the draining popliteal lymph nodes were harvested in RNAlater solution (Ambion) before subsequent RNA extraction and qPCR analysis.

MicroWestern Arrays

The MicroWestern Array (MWA) method previously described (Ciaccio et al., 2010) was modified to accommodate a larger number of lysates.

Phosphotyrosine and global phospopeptide analysis

Tyrosine-phosphorylated peptides from BMDC lysates were prepared using a PhosphoScan Kit (Cell Signaling Technology), and analyzed by data-dependent LC-MS/MS using a Thermo LTQ-Orbitrap. Quantitative analysis of serine, threonine, and tyrosine phosphorylated peptides was performed using SCX/IMAC as described (Villen and Gygi, 2008) with some modifications. Peptide samples were analyzed on a LTQ Orbitrap Velos (Thermo Fisher Scientific). To identify and quantify peptides, mass spectra were processed with Spectrum Mill software package (Agilent Technologies) v4.0b, including in-house developed features for SILAC quantitation and phosphosite localization, and with

MaxQuant (v1.0.13.13) (Cox and Mann, 2008) and Mascot search engine (v2.2.0, Matrix Science).

Supplementary Material

Refer to Web version on PubMed Central for supplementary material.

Acknowledgments

We thank the members of the Hacohen and Regev laboratories, O. Takeuchi, B. Beutler, D. Mathis, P. Anderson, L. Glimcher, and D. Bartel for valuable discussions and comments; L. Gaffney and L. Solomon for assistance with figures and artwork; and S. Gupta and the Broad Genetic Analysis Platform for microarray processing. Supported by NIH grant U54 AI057159, the NIH New Innovator Award DP2 OD002230 (N.H.) and NIH P50 HG006193 (A.R., N.H.); a Ph.D fellowship from the Boehringer Ingelheim Fonds (N.C.); the Human Frontier Science Program Organization and a Claire and Emanuel G. Rosenblatt Award from the American Physicians Fellowship for Medicine in Israel (I.A.); NIH Pioneer Awards (A.R., H.P.); and by a Career Award at the Scientific Interface from the Burroughs Wellcome Fund, the Sloan Foundation and HHMI (A.R.). A.R. is an investigator of the Merkin Foundation for Stem Cell Research at the Broad Institute. This work was partially supported by a pilot award from the NIH Chicago Center for Systems Biology P50 GM081892-03 to R.B.J.; and an award from the American Cancer Society Illinois Division to R.B.J.

REFERENCES

Amit I, Citri A, Shay T, Lu Y, Katz M, Zhang F, Tarcic G, Siwak D, Lahad J, Jacob-Hirsch J, et al. A module of negative feedback regulators defines growth factor signaling. Nat Genet. 2007; 39:503–512. [PubMed: 17322878]

Amit I, Garber M, Chevrier N, Leite AP, Donner Y, Eisenhaure T, Guttman M, Grenier JK, Li W, Zuk O, et al. Unbiased reconstruction of a mammalian transcriptional network mediating pathogen responses. Science. 2009; 326:257–263. [PubMed: 19729616]

Archambault V, Glover DM. Polo-like kinases: conservation and divergence in their functions and regulation. Nat Rev Mol Cell Biol. 2009; 10:265–275. [PubMed: 19305416]

Banchereau J, Pascual V. Type I interferon in systemic lupus erythematosus and other autoimmune diseases. Immunity. 2006; 25:383–392. [PubMed: 16979570]

Barbie DA, Tamayo P, Boehm JS, Kim SY, Moody SE, Dunn IF, Schinzel AC, Sandy P, Meylan E, Scholl C, et al. Systematic RNA interference reveals that oncogenic KRAS-driven cancers require TBK1. Nature. 2009; 462:108–112. [PubMed: 19847166]

Barrat FJ, Coffman RL. Development of TLR inhibitors for the treatment of autoimmune diseases. Immunol Rev. 2008; 223:271–283. [PubMed: 18613842]

Birge RB, Kalodimos C, Inagaki F, Tanaka S. Crk and CrkL adaptor proteins: networks for physiological and pathological signaling. Cell Commun Signal. 2009; 7:13. [PubMed: 19426560]

Blasius AL, Beutler B. Intracellular toll-like receptors. Immunity. 2010; 32:305–315. [PubMed: 20346772]

Chang J, Cizmecioglu O, Hoffmann I, Rhee K. PLK2 phosphorylation is critical for CPAP function in procentriole formation during the centrosome cycle. EMBO J. 2010; 29:2395–2406. [PubMed: 20531387]

Chien Y, Kim S, Bumeister R, Loo YM, Kwon SW, Johnson CL, Balakireva MG, Romeo Y, Kopelovich L, Gale M Jr. et al. RalB GTPase-mediated activation of the IkappaB family kinase TBK1 couples innate immune signaling to tumor cell survival. Cell. 2006; 127:157–170. [PubMed: 17018283]

Chu WM, Ostertag D, Li ZW, Chang L, Chen Y, Hu Y, Williams B, Perrault J, Karin M. JNK2 and IKKbeta are required for activating the innate response to viral infection. Immunity. 1999; 11:721–731. [PubMed: 10626894]

Ciaccio MF, Wagner JP, Chuu CP, Lauffenburger DA, Jones RB. Systems analysis of EGF receptor signaling dynamics with microwestern arrays. Nat Methods. 2010; 7:148–155. [PubMed: 20101245]

Cizmecioglu O, Warnke S, Arnold M, Duensing S, Hoffmann I. Plk2 regulated centriole duplication is dependent on its localization to the centrioles and a functional polo-box domain. Cell Cycle. 2008; 7:3548–3555. [PubMed: 19001868]

Cox J, Mann M. MaxQuant enables high peptide identification rates, individualized p.p.b.-range mass accuracies and proteome-wide protein quantification. Nat Biotechnol. 2008; 26:1367–1372. [PubMed: 19029910]

Crozat K, Hoebe K, Ugolini S, Hong NA, Janssen E, Rutschmann S, Mudd S, Sovath S, Vivier E, Beutler B. Jinx, an MCMV susceptibility phenotype caused by disruption of Unc13d: a mouse model of type 3 familial hemophagocytic lymphohistiocytosis. J Exp Med. 2007; 204:853–863. [PubMed: 17420270]

Doyle S, Vaidya S, O'Connell R, Dadgostar H, Dempsey P, Wu T, Rao G, Sun R, Haberland M, Modlin R, et al. IRF3 mediates a TLR3/TLR4-specific antiviral gene program. Immunity. 2002; 17:251–263. [PubMed: 12354379]

Fraser ID, Germain RN. Navigating the network: signaling cross-talk in hematopoietic cells. Nat Immunol. 2009; 10:327–331. [PubMed: 19295628]

Freeman M. Feedback control of intercellular signalling in development. Nature. 2000; 408:313–319. [PubMed: 11099031]

Heikkinen LS, Kazlauskas A, Melen K, Wagner R, Ziegler T, Julkunen I, Saksela K. Avian and 1918 Spanish influenza a virus NS1 proteins bind to Crk/CrkL Src homology 3 domains to activate host cell signaling. J Biol Chem. 2008; 283:5719–5727. [PubMed: 18165234]

Hennessy EJ, Parker AE, O'Neill LA. Targeting Toll-like receptors: emerging therapeutics? Nat Rev Drug Discov. 2010; 9:293–307. [PubMed: 20380038]

Hrincius ER, Wixler V, Wolff T, Wagner R, Ludwig S, Ehrhardt C. CRK adaptor protein expression is required for efficient replication of avian influenza A viruses and controls JNK-mediated apoptotic responses. Cell Microbiol. 2010; 12:831–843. [PubMed: 20088952]

Iannacone M, Moseman EA, Tonti E, Bosurgi L, Junt T, Henrickson SE, Whelan SP, Guidotti LG, von Andrian UH. Subcapsular sinus macrophages prevent CNS invasion on peripheral infection with a neurotropic virus. Nature. 2010; 465:1079–1083. [PubMed: 20577213]

Kawagoe T, Takeuchi O, Takabatake Y, Kato H, Isaka Y, Tsujimura T, Akira S. TANK is a negative regulator of Toll-like receptor signaling and is critical for the prevention of autoimmune nephritis. Nat Immunol. 2009; 10:965–972. [PubMed: 19668221]

Keller AD, Maniatis T. Identification and characterization of a novel repressor of beta-interferon gene expression. Genes Dev. 1991; 5:868–879. [PubMed: 1851123]

Kuan AP, Chamberlain W, Malkiel S, Lieu HD, Factor SM, Diamond B, Kotzin BL. Genetic control of autoimmune myocarditis mediated by myosin-specific antibodies. Immunogenetics. 1999; 49:79–85. [PubMed: 9887344]

Matsui K, Kumagai Y, Kato H, Sato S, Kawagoe T, Uematsu S, Takeuchi O, Akira S. Cutting edge: Role of TANK-binding kinase 1 and inducible IkappaB kinase in IFN responses against viruses in innate immune cells. J Immunol. 2006; 177:5785–5789. [PubMed: 17056502]

Mross K, Frost A, Steinbild S, Hedbom S, Rentschler J, Kaiser R, Rouyrre N, Trommeshauser D, Hoesl CE, Munzert G. Phase I dose escalation and pharmacokinetic study of BI 2536, a novel Polo-like kinase 1 inhibitor, in patients with advanced solid tumors. J Clin Oncol. 2008; 26:5511–5517. [PubMed: 18955456]

Ong SE, Blagoev B, Kratchmarova I, Kristensen DB, Steen H, Pandey A, Mann M. Stable isotope labeling by amino acids in cell culture, SILAC, as a simple and accurate approach to expression proteomics. Mol Cell Proteomics. 2002; 1:376–386. [PubMed: 12118079]

Reizis B, Bunin A, Ghosh HS, Lewis KL, Sisirak V. Plasmacytoid dendritic cells: recent progress and open questions. Annu Rev Immunol. 2011; 29:163–183. [PubMed: 21219184]

Rothlin CV, Ghosh S, Zuniga EI, Oldstone MB, Lemke G. TAM receptors are pleiotropic inhibitors of the innate immune response. Cell. 2007; 131:1124–1136. [PubMed: 18083102]

Santiago-Raber ML, Baccala R, Haraldsson KM, Choubey D, Stewart TA, Kono DH, Theofilopoulos AN. Type-I interferon receptor deficiency reduces lupus-like disease in NZB mice. J Exp Med. 2003; 197:777–788. [PubMed: 12642605]

Seeburg DP, Pak D, Sheng M. Polo-like kinases in the nervous system. Oncogene. 2005; 24:292–298. [PubMed: 15640845]

Shalek AK, Robinson JT, Karp ES, Lee JS, Ahn DR, Yoon MH, Sutton A, Jorgolli M, Gertner RS, Gujral TS, et al. Vertical silicon nanowires as a universal platform for delivering biomolecules into living cells. Proc Natl Acad Sci U S A. 2010; 107:1870–1875. [PubMed: 20080678]

Sharma K, Kumar C, Keri G, Breitkopf SB, Oppermann FS, Daub H. Quantitative analysis of kinase-proximal signaling in lipopolysaccharide-induced innate immune response. J Proteome Res. 2010; 9:2539–2549. [PubMed: 20222745]

Strebhardt K. Multifaceted polo-like kinases: drug targets and antitargets for cancer therapy. Nat Rev Drug Discov. 2010; 9:643–660. [PubMed: 20671765]

Takayanagi H, Kim S, Matsuo K, Suzuki H, Suzuki T, Sato K, Yokochi T, Oda H, Nakamura K, Ida N, et al. RANKL maintains bone homeostasis through c-Fos-dependent induction of interferon-beta. Nature. 2002; 416:744–749. [PubMed: 11961557]

Takeuchi O, Akira S. Pattern recognition receptors and inflammation. Cell. 2010; 140:805–820. [PubMed: 20303872]

Villen J, Gygi SP. The SCX/IMAC enrichment approach for global phosphorylation analysis by mass spectrometry. Nat Protoc. 2008; 3:1630–1638. [PubMed: 18833199]

Vitour D, Dabo S, Ahmadi Pour M, Vilasco M, Vidalain PO, Jacob Y, Mezel-Lemoine M, Paz S, Arguello M, Lin R, et al. Polo-like kinase 1 (PLK1) regulates interferon (IFN) induction by MAVS. J Biol Chem. 2009; 284:21797–21809. [PubMed: 19546225]

Wang L, Gordon RA, Huynh L, Su X, Park Min KH, Han J, Arthur JS, Kalliolias GD, Ivashkiv LB. Indirect inhibition of Toll-like receptor and type I interferon responses by ITAM-coupled receptors and integrins. Immunity. 2010; 32:518–530. [PubMed: 20362473]

Weintz G, Olsen JV, Fruhauf K, Niedzielska M, Amit I, Jantsch J, Mages J, Frech C, Dolken L, Mann M, et al. The phosphoproteome of toll-like receptor-activated macrophages. Mol Syst Biol. 2010; 6:371. [PubMed: 20531401]

Wellcome Trust Case Control Consortium. Genome-wide association study of 14,000 cases of seven common diseases and 3,000 shared controls. Nature. 2007; 447:661–678. [PubMed: 17554300]

Xiao N, Eidenschenk C, Krebs P, Brandl K, Blasius AL, Xia Y, Khovananth K, Smart NG, Beutler B. The Tpl2 mutation Sluggish impairs type I IFN production and increases susceptibility to group B streptococcal disease. J Immunol. 2009; 183:7975–7983. [PubMed: 19923465]

Ye J, Chen S, Maniatis T. Cardiac glycosides are potent inhibitors of interferon-beta gene expression. Nat Chem Biol. 2011; 7:25–33. [PubMed: 21076398]

Zhang W, Wang J, Zhang Y, Yuan Y, Guan W, Jin C, Chen H, Wang X, Yang X, He F. The scaffold protein TANK/I-TRAF inhibits NF-kappaB activation by recruiting polo-like kinase 1. Mol Biol Cell. 2010; 21:2500–2513. [PubMed: 20484576]

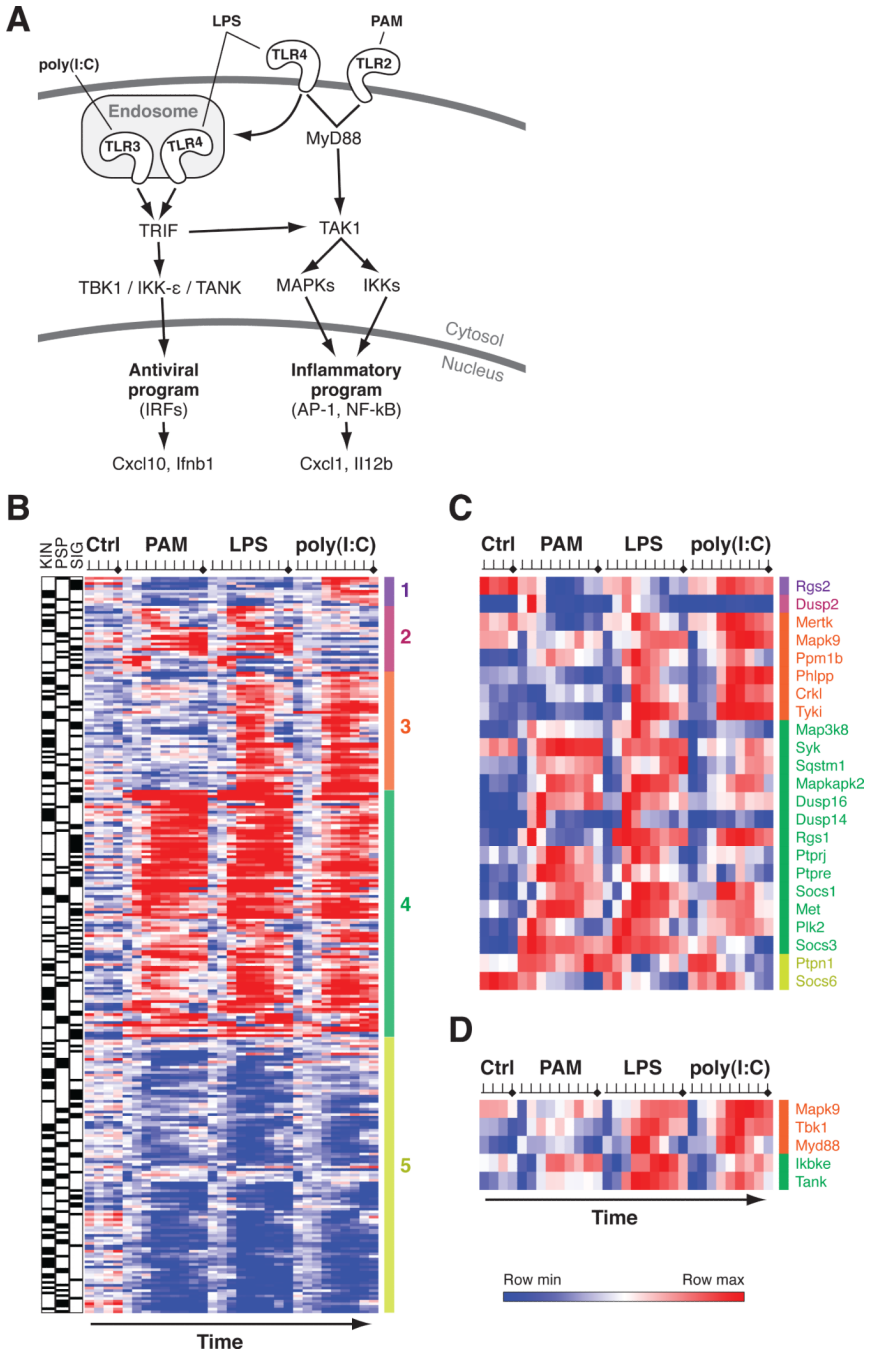

Figure 1. mRNAs of signaling components are differentially regulated upon Toll-like receptor (TLR) stimulation

(A) Simplified schematic of the TLR2, 3, and 4 pathways (Takeuchi and Akira, 2010). (B) mRNA expression profiles of differentially expressed signaling genes. Shown are expression profiles for 280 differentially expressed signaling genes (rows) at different time points (columns): a control time course (no stimulation, Ctrl) and following stimulations with Pam3CSK4 (PAM), lipopolysaccharide (LPS), and poly(I:C). Tick marks: time point post-stimulation (0.5, 1, 2, 4, 6, 8, 12, 16, 24 h). Shown are genes with at least a 1.7 fold change in expression compared to pre-stimulation levels in both duplicates of at least one time point. The three leftmost columns indicate kinase (KIN), phosphatase (PSP), and

signaling regulators (SIG) (black bars). Values from duplicate arrays were collapsed and gene expression profiles were hierarchically clustered. The rightmost color-coded column indicates the 5 major expression clusters.
(C and D) mRNA expression profiles of candidate (C) and canonical (D) TLR signaling regulators selected for subsequent experiments. The color-coding of the gene names highlight the corresponding expression cluster from the complete matrix from A.
See also **Table S1**.

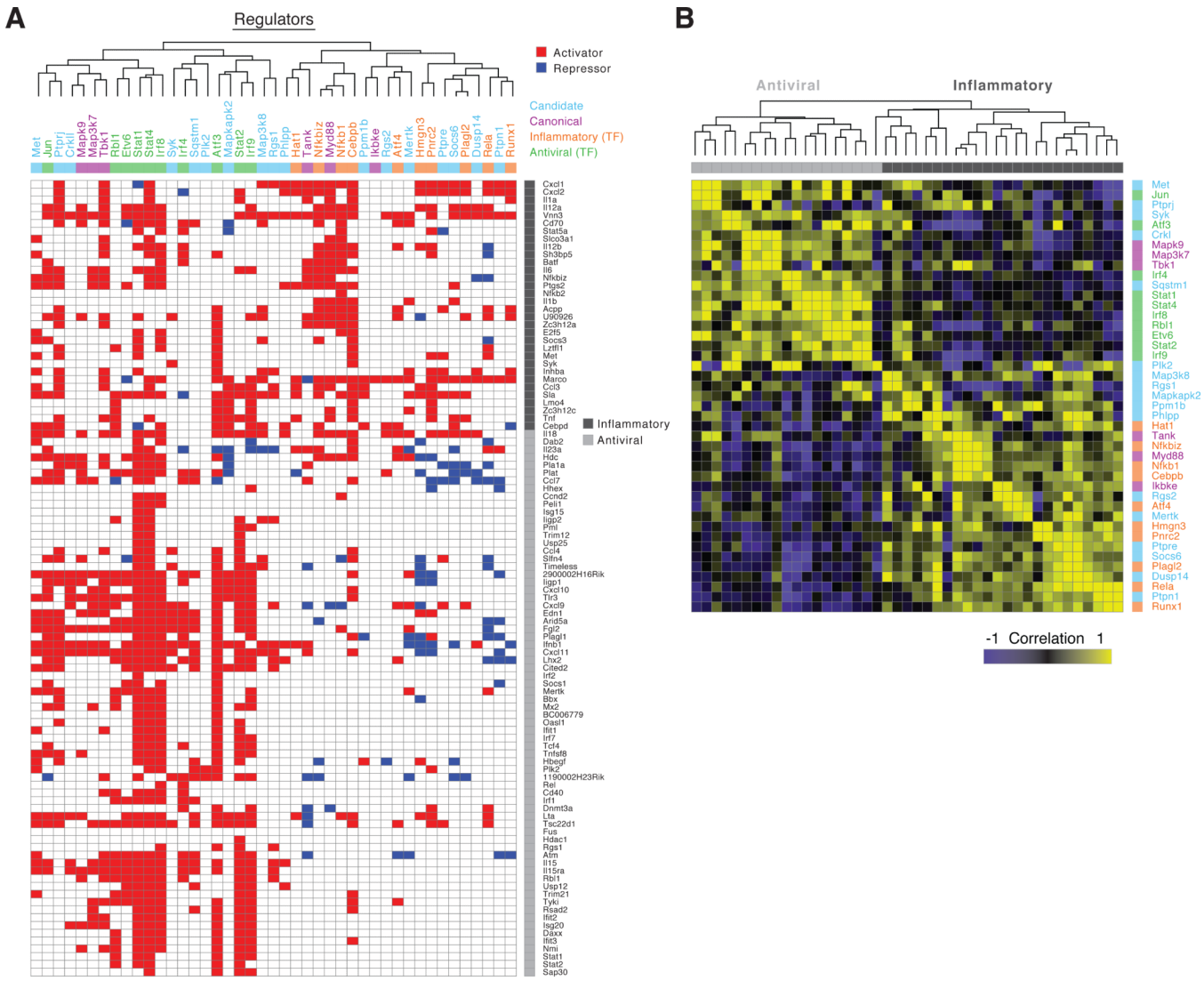

Figure 2. A perturbation strategy assigns function to signaling components within the TLR pathways

(A) Perturbation profiles of six canonical (purple) and 17 candidate (blue) signaling components, and 20 core TLR transcriptional regulators belonging to the inflammatory (orange) and the antiviral (green) programs. Shown are the perturbed regulators (columns) and their statistically significant effects (False discovery rate, FDR < 0.02) on each of the 118 TLR signature genes (rows). Red: significant activating relation (target gene expression decreased following perturbation); blue: significant repressing relation (target gene expression increased following perturbation); white: no significant effect. The right-most column categorizes signature genes into antiviral (light grey) and inflammatory (dark grey) programs.

(B) Functional characterization based on similarity of perturbation profiles. Shown is a correlation matrix of the perturbation profiles from A. Yellow: positive correlation; purple: negative correlation; black: no correlation.

See also **Figure S1 and S2**, and **Table S2**.

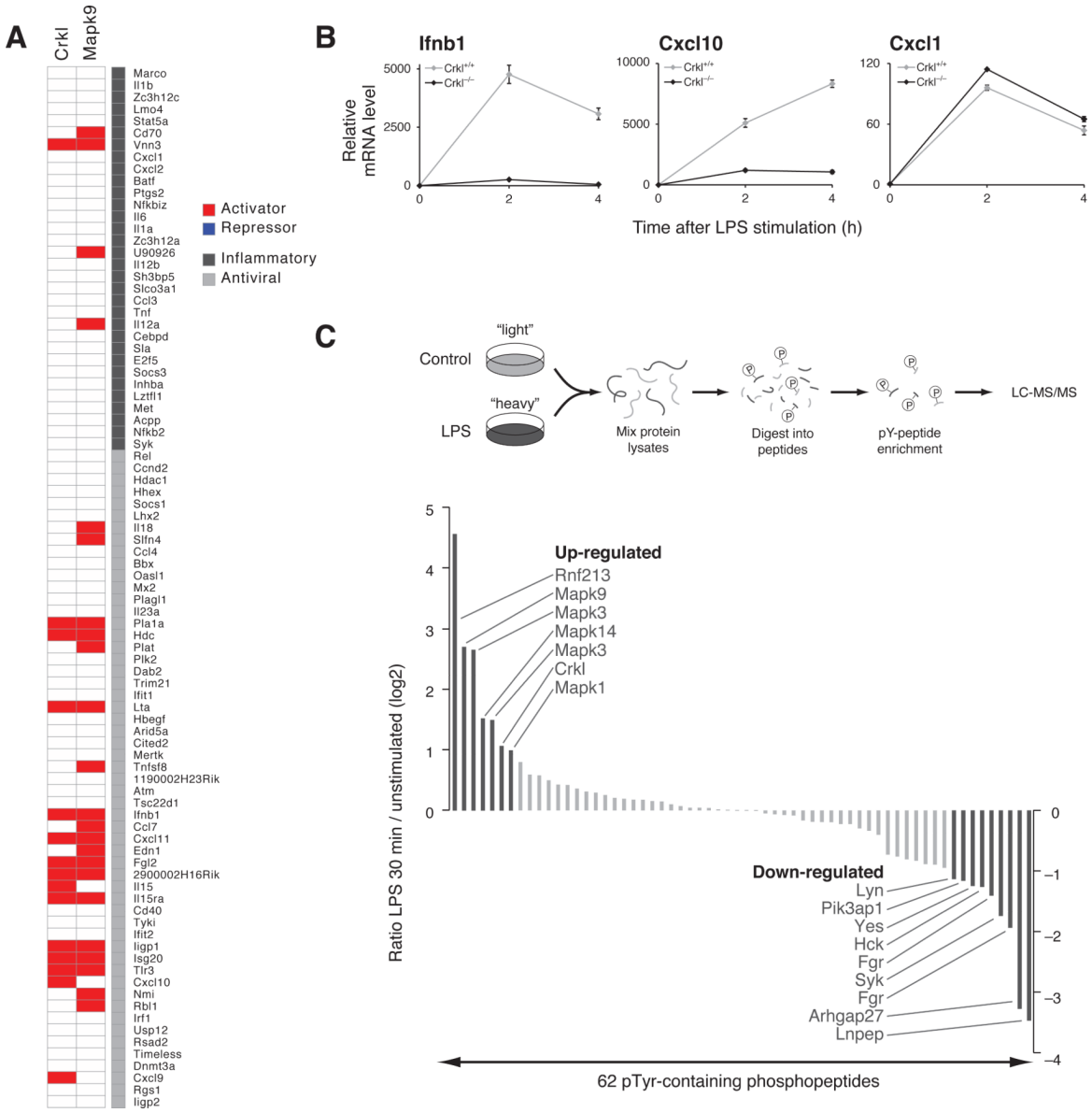

Figure 3. Crkl adaptor functions in the antiviral arm of TLR4 signaling

(A) Comparison of Crkl and Mapk9 knockdown profiles. Shown are the effects of Crkl and Mapk9 perturbation (columns) on the 118 signature genes (rows). Data was extracted from **Figure 2A**.

(B) Inhibition of transcription of antiviral cytokines in Crkl$^{-/-}$ BMDCs. Shown are mRNA levels (qPCR; relative to t = 0) for Ifnb1 (left), Cxcl10 (middle) and Cxcl1 (right) in three replicates per time point. Error bars represent the SEM (n = 3 mice).

(C) Crkl phosphorylation is induced following LPS stimulation. **Top**: Schematic depiction of experimental workflow. From left: Protein lysates from unstimulated (Control) and LPS-treated BMDCs grown in "light" and "heavy" SILAC medium were mixed (1:1) and digested into peptides with trypsin before phospho-tyrosine (pY) peptide enrichment by immunoprecipitation, and LC-MS/MS analysis. **Bottom**: Shown are the differential phosphorylation levels (log 2 ratios, Y axis) of all 62 phosphopeptides identified and quantified by LC-MS/MS (X axis). Black: peptides with more than 2 fold differential expression (left: induced; right: repressed).

See also **Table S3**.

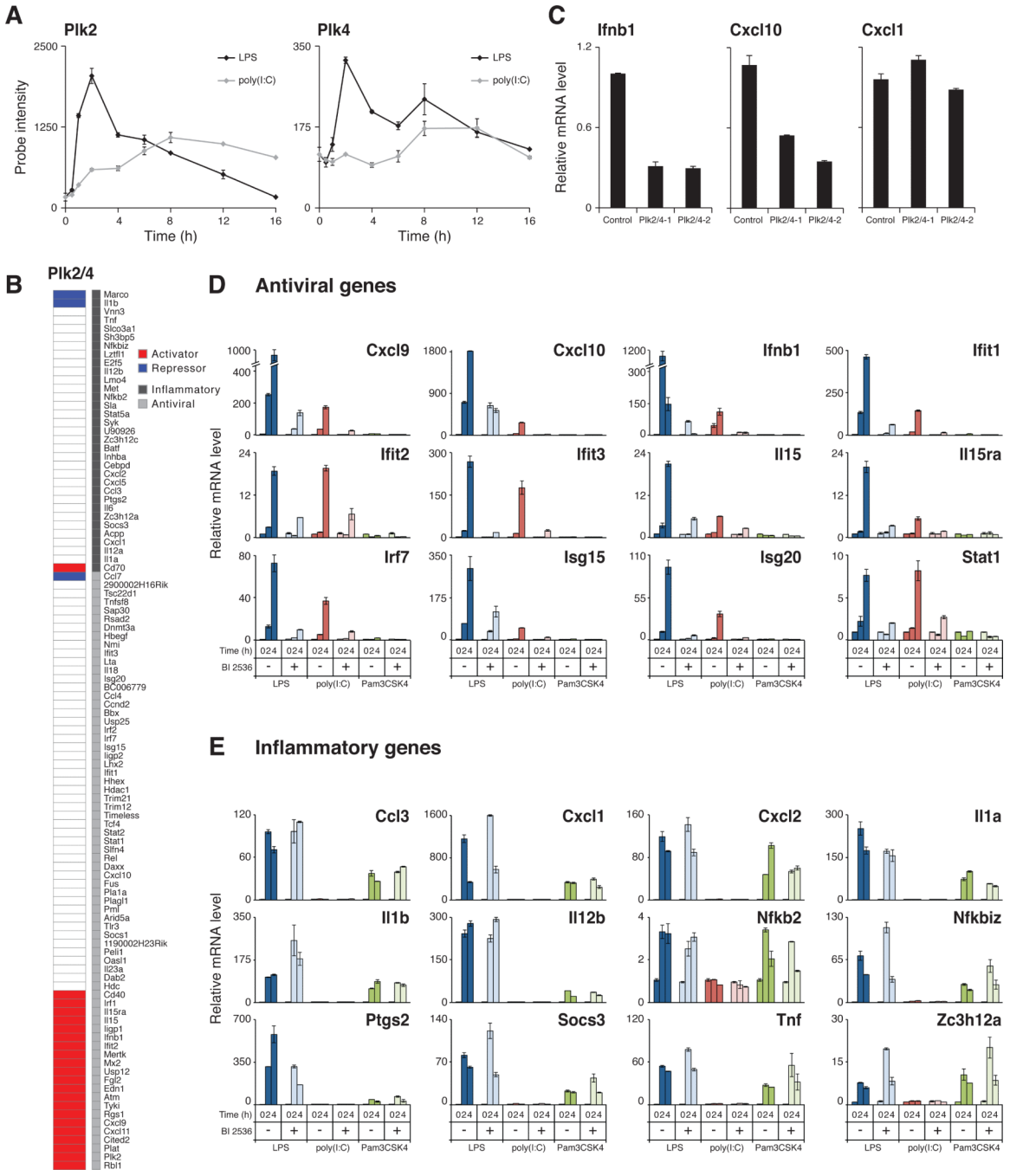

Figure 4. Polo-like kinase (Plk) 2 and 4 regulate the antiviral program

(A) Similarity of Plk2 and Plk4 mRNA expression profiles. Shown are mRNA levels (from **Figure 1B**) of Plk2 (left) and Plk4 (right) following stimulation with LPS (black) or poly(I:C) (grey).

(B) Double knockdown of Plk2 and 4 represses the antiviral signature. Shown are significant changes in expression of TLR signature genes (rows) following double knockdown of Plk2 and 4. Red and blue mark significant hits as in **Figure 2**, only for genes where the effect was consistent between the two independent combinations of shRNAs.

(C) Double knockdown of Plk2 and 4 represses antiviral cytokine mRNAs. Shown are expression levels (qPCR) relative to control shRNAs (Control) for two antiviral cytokines (Ifnb1 and Cxcl10) and for an inflammatory cytokine (Cxcl1), following LPS stimulation in BMDCs using two independent combinations of shRNAs (Plk2/4-1, Plk2/4-2). Three replicates for each experiment; error bars are the SEM.
(D and E) BI 2536 specifically abrogates transcription of antiviral genes without affecting inflammatory genes following stimulation with LPS, poly(I:C), or Pam3CSK4. Shown are mRNA levels (qPCR; relative to t = 0) for 12 indicated antiviral (D) and 12 inflammatory (E) genes in BMDCs treated with BI 2536 (1 μM; dark color bars) or DMSO vehicle (light color bars) and stimulated for 0, 2 or 4 h with LPS (dark and light See also **Figures S3 and S4** and **Table S4**.

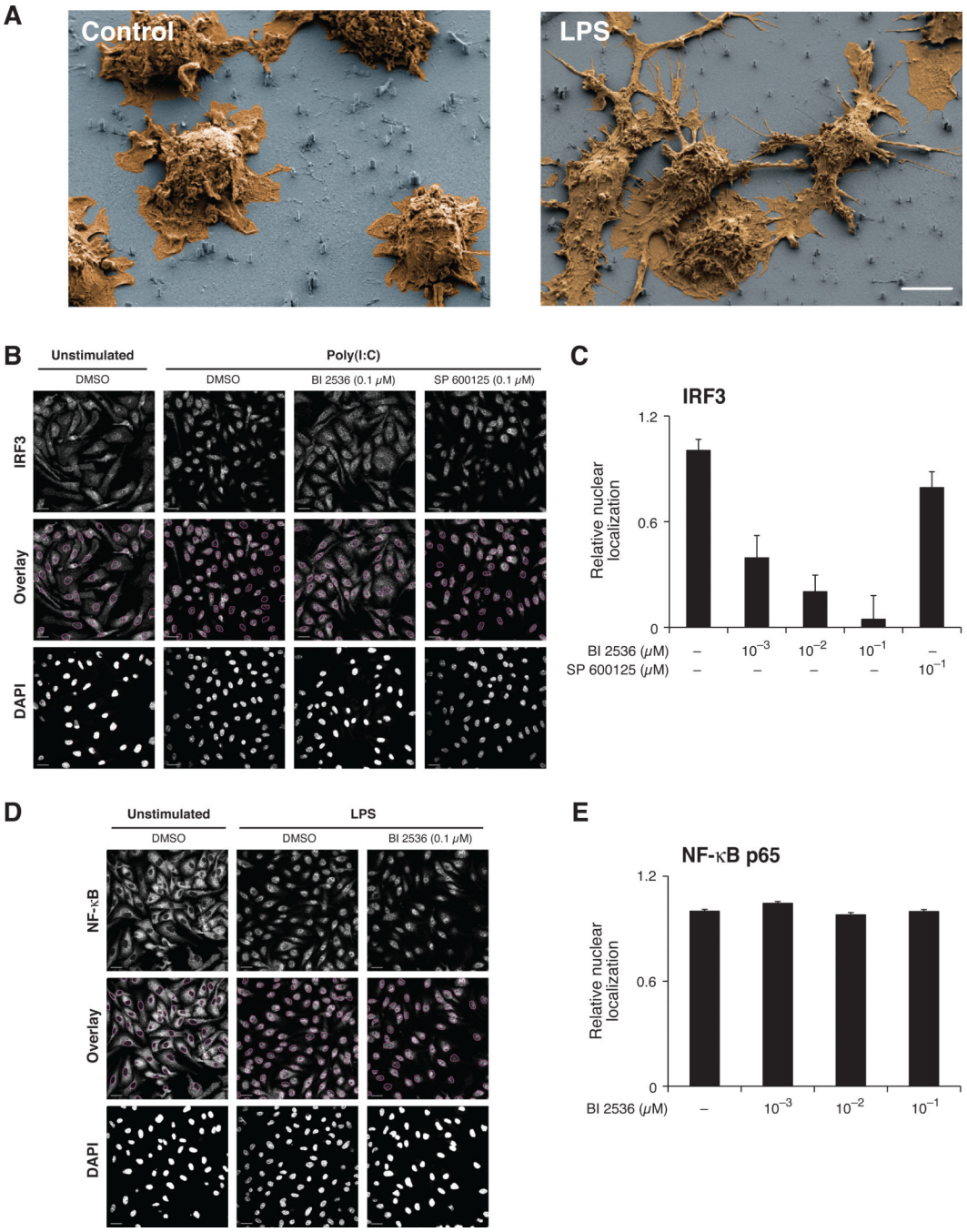

Figure 5. BI 2536-mediated Plk inhibition blocks IRF3 nuclear translocation in DCs

(A) DCs on nanowires (NW) undergo normal morphological changes upon LPS stimulation. Shown are electron micrographs of BMDCs plated on bare vertical silicon NW that were left unstimulated (left; Control) or stimulated with LPS (right). Scale bars, 5 μm.

(B-E) BI 2536 inhibits IRF3, but not NF-κB p65, nuclear translocation following TLR stimulation. (B and D) Shown are confocal micrographs of BMDCs plated on vertical silicon NW pre-coated with vehicle control (DMSO; B and D), Plk inhibitor (BI 2536; B and D), or control Jnk inhibitor (SP 600125; B), and stimulated with poly(I:C) for 2 h (B) or LPS for 30 min (D) (reflecting peak time of nuclear translocation for IRF3 and NF-κB p65, respectively), or left unstimulated (B and D). Cells were analyzed for DAPI (B and D), IRF3

(B) and NF-κB p65 subunit (D) staining. Scale bars, 5 μM. (C and E) Nuclear translocation (from confocal micrographs) of IRF3 (C) and NF-κB p65 (E) was quantified using DAPI staining as a nuclear mask (purple circles; overlay in B and D) to determine the ratio of total versus nuclear fluorescence (Y axis) in BMDCs cultured on NW coated with different amounts of BI 2536 or SP 600125, or with vehicle control (DMSO; X axis). Three replicates in each experiment; error bars are the SEM.
See also **Figure S5**.

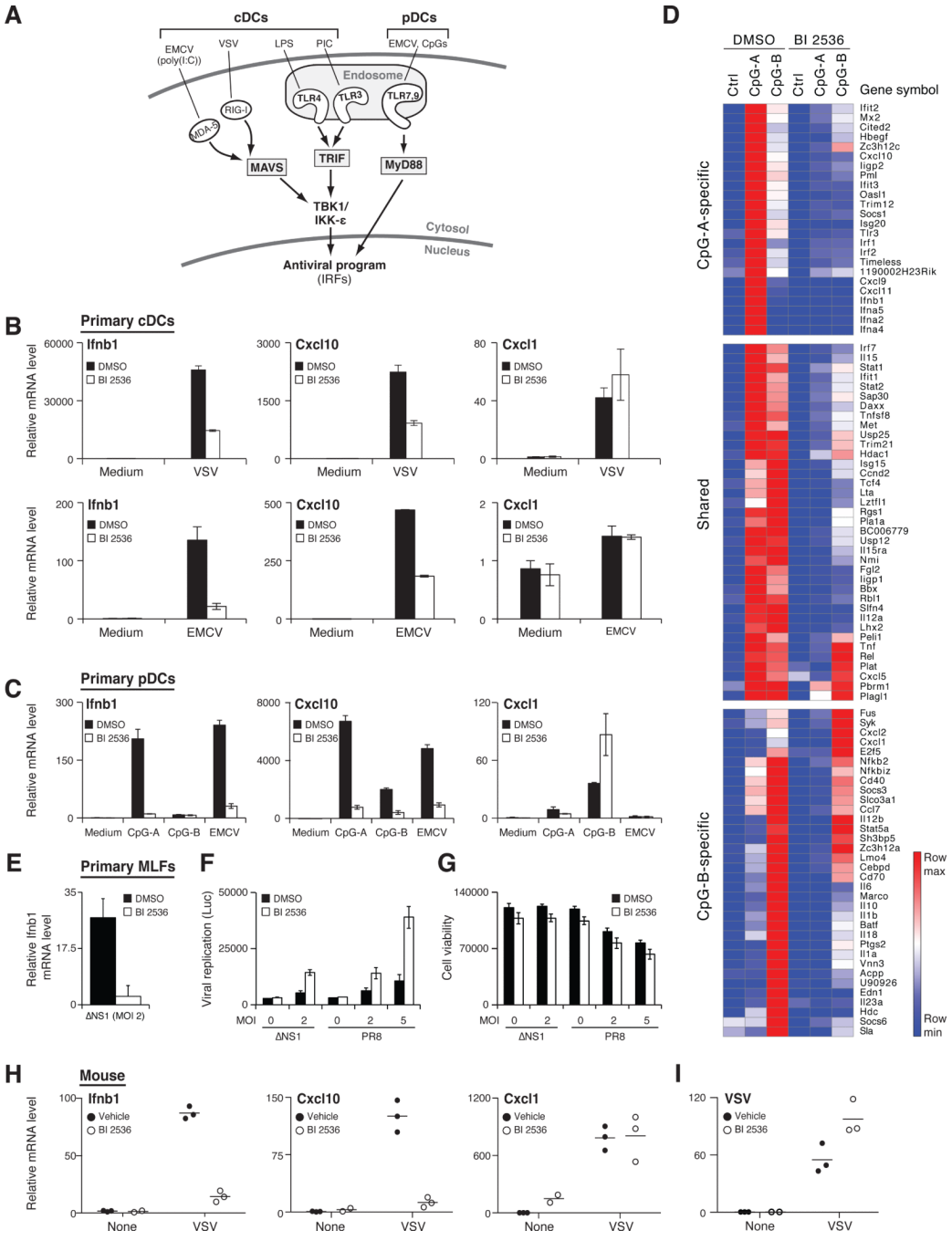

Figure 6. Plks are critical in the induction of type I interferons *in vitro* and *in vivo*

(A) IFN-inducing pathways in conventional DCs (cDCs) and plasmacytoid DCs (pDCs).

(B, C) BI 2536 inhibits mRNA levels for antiviral cytokines in response to diverse stimuli in cDCs and pDCs. Shown are Ifnb1, Cxcl10 and Cxcl1 mRNA levels (qPCR; relative to t = 0) in cells treated with BI 2536 (1 μM; white bars) or DMSO vehicle (black bars) in cDCs (B) infected with VSV (MOI 1; B top) or with EMCV (MOI 10; B bottom), and in pDCs (C) stimulated with CpG type A or B, or infected with EMCV (MOI 10). Three replicates in each experiment; error bars are the SEM.

(D) BI 2536 inhibits the CpG-A response, but has little effect on the CpG-B response. Shown are mRNA levels (nCounter) for the 118 TLR signature genes (rows) in pDCs

treated with DMSO vehicle or BI 2536 (1 μM) and left untreated (Ctrl) or stimulated with CpG-A or -B for 6 h (columns). Three clusters of genes are shown: CpG-A-specific (top), CpG-B-specific (bottom), and shared by CpG-A and -B (middle).

(E-G) BI 2536 inhibits IFN-β production in primary mouse lung fibroblasts (MLFs), leading to an increase in viral replication. MLFs treated with BI 2536 (1 μM; white bars) or vehicle control (DMSO; black bars) were infected with influenza ΔNS1 or PR8 strains at indicated MOIs. Shown are Ifnb1 mRNA levels measured by qPCR (relative to t = 0; E), viral replication as measured by luciferase (Luc) activity in reporter cells (F), and cell viability measured by CellTiter-Glo assay (G).

(H and I) BI 2536 inhibits antiviral cytokine mRNA production, while increasing viral replication during *in vivo* VSV infection. Shown are Ifnb1, Cxcl10 and Cxcl1 mRNA (H), and VSV viral RNA (I) levels (qPCR; relative to uninfected animals) from popliteal lymph nodes of mice injected with BI 2536 (white circles) or DMSO vehicle (black circles) prior to and during the course of infection with VSV (intra-footpad). Nodes were harvested six hours post-infection. Each circle represents one animal (n = 3). Data is representative of three independent experiments for each condition.

See also **Figure S6** and **Table S5**.

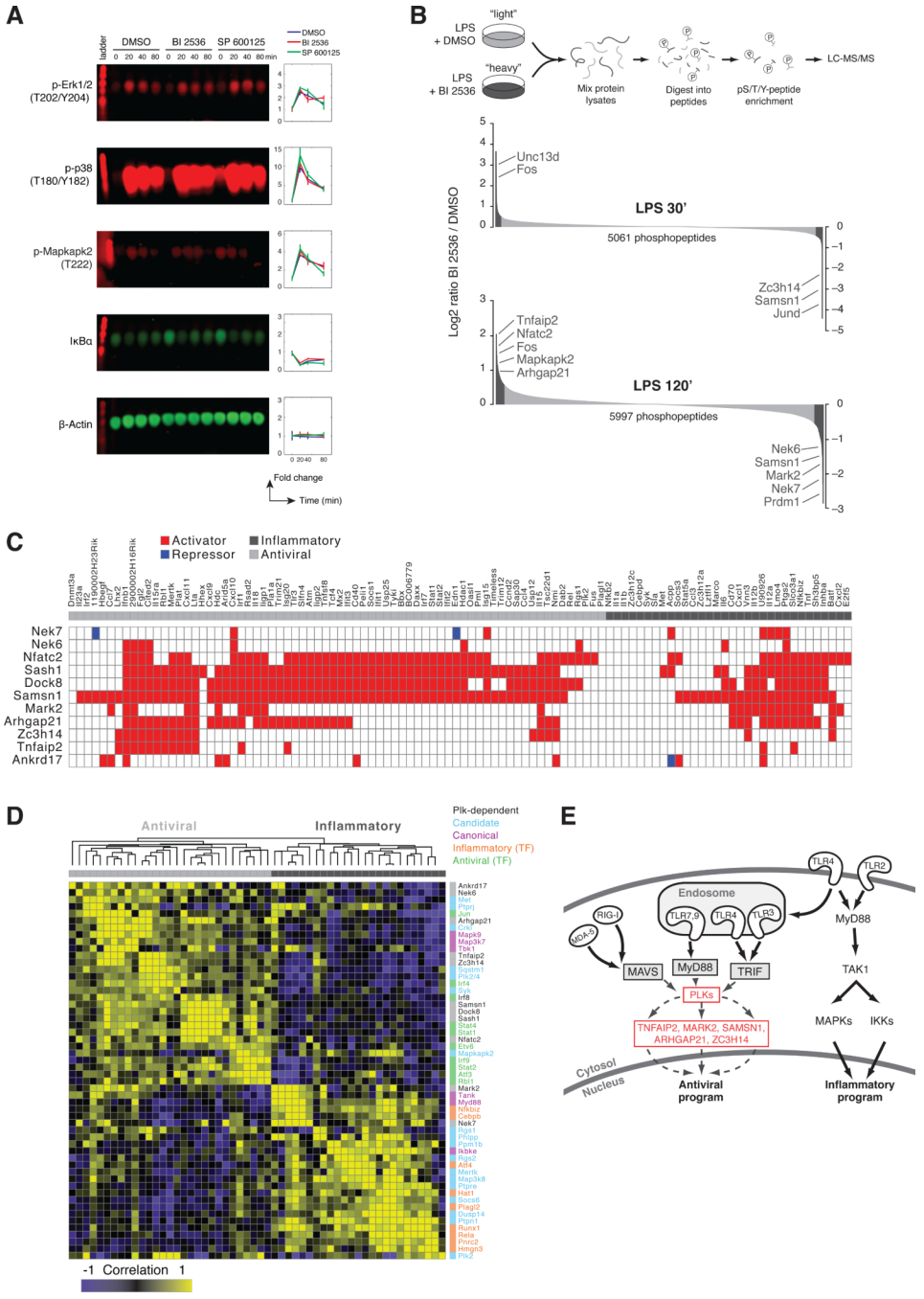

Figure 7. Unbiased phosphoproteomics identifies a Plk-dependent antiviral pathway

(A) BI 2536 does not affect phosphorylation and protein levels of known TLR signaling nodes. Shown are representative MicroWestern Array (MWA; see Experimental Procedures) blots (left) obtained from analyzing lysates from BMDCs pre-treated with DMSO, BI 2536 (1 μM), or SP 600125 (5 μM) and stimulated with LPS for 0, 20, 40, 80 min. Blots were analyzed using indicated antibodies (left most), and fold change in fluorescence signals was quantified relative to t = 0 (right). Error bars are the SEM of triplicate MWA blots.

(B) BI 2536 affects protein phosphorylation levels during LPS stimulation. **Top:** Schematic depiction of experimental workflow. From left to right: LPS-stimulated BMDCs cultured in "heavy" or "light" SILAC medium were pre-treated with BI 2536 (1 μM) or DMSO,

respectively. Protein lysates were mixed (1:1) and digested into peptides with trypsin, before phospho-serine, -threonine and -tyrosine (pS/T/Y) peptide enrichment, and LC-MS/MS analysis. **Bottom:** Shown are the differential phosphorylation levels (average $\log_2$ ratios of two independent experiments; Y axis) of all 5061 and 5997 phosphopeptides respectively identified and quantified by LC-MS/MS (X axis) at 30 min (top) and 120 min (bottom) post-LPS stimulation. Dark grey: phosphopeptides with a significant change ($P_{unadjusted} < 0.001$ for both time points; $FDR_{30min} = 0.05$; $FDR_{120min} = 0.03$; left: induced; right: repressed). Average ratios from phosphopeptides identified and quantified in two independent experiments are depicted. (C) Eleven Plk-dependent phosphoproteins significantly affect the expression of TLR signature genes. Shown are significant changes in expression of the TLR signature genes (rows) following knockdown of each of the 11 phosphoproteins (columns), following stimulation with LPS for 6 h. Red and blue mark significant hits (as presented in **Figure 2**) and are shown only for genes where the effect was consistent between two independent experiments.

(D) Functional characterization based on similarity of perturbation profiles. Shown is a correlation matrix of the perturbation profiles from C (grey), and those from Figure 2B including canonical (purple) and candidate (blue) signaling components as well as core antiviral (green) and inflammatory (orange) transcriptional regulators. Yellow: positive correlation; purple: negative correlation; black: no correlation.

(E) A Plk-dependent pathway in antiviral sensing. Shown is a diagram of a model of the Plk-dependent pathway of IFN induction in innate immunity. Out of the 11 Plk-dependent proteins described in C and D, only the 5 showing a phenotype with 2 independent shRNAs are depicted.

See also **Figure S7** and **Tables S6 and S7**.